Annals of Medical and Clinical Oncology
Zhao Z, et al. Ann med clin Oncol 6: 144.
www.doi.org/10.29011/2833-3497.000144
www.gavinpublishers.com

OPEN ACCESS

GAVIN PUBLISHERS

Research Article

Differential Expression of Necroptosis-Related Genes with regulating lncRNA in Triple Negative Breast Cancer to Predict Prognosis and Immunotherapy Response

Zijun Zhao[1#], Xiayao Diao[1#], Qing Cao[1], Xin Lu[1*]

[1]Department of Surgery, Peking Union Medical College Hospital, Chinese Academy of Medical Sciences and Peking Union Medical College, Beijing, China.

[*]**Corresponding author:** Xin Lu, Professor, Department of Surgery, Peking Union Medical College Hospital, Chinese Academy of Medical Sciences and Peking Union Medical College, 1 Shuaifuyuan, Wangfujing, Beijing 100730, China.

[#] ZJZ and XYD contributed equally to this work

Citation: Zhao Z, Diao X, Cao Q, Lu X (2023) Differential Expression of Necroptosis-Related Genes with regulating lncRNA in Triple Negative Breast Cancer to Predict Prognosis and Immunotherapy Response. Ann med clin Oncol 5: 144. DOI: https://doi.org/10.29011/2833-3497.000144

Received Date: 02 February, 2023; **Accepted Date:** 08 February, 2023; **Published Date:** 10 February, 2023

Abstract

Purpose: Necroptosis is essential in tumor biology in which lncRNAs play an important role but related studies in triple negative breast cancer (TNBC) were insufficient. We aim to screen remarkable necroptosis-related lncRNA and construct a lncNRA-related risk model for precision of immunotherapy. **Methods**: Transcriptional data were acquired from TCGA database. Differentially expressed genes (DEGs) related to necroptosis were obtained in TNBC samples. LncRNAs related to DEGs were analyzed by following Cox and least absolute shrinkage and selection operator regression analysis. Prognosis-associated lncRNAs were brought into a model which divided training and testing samples into high-/low-risk subgroups. Survival analysis between these subgroups were conducted and independent variables of prognosis were selected. Nomogram was then created to predict prognosis of selected patients. Comparisons of immune landscape, tumor microenvironment, and immunotherapy response were performed between the two subgroups. **Results**: Seven necroptosis-related DEGs (NRGs) were found in TNBC. Six of 153 NRG-related lncRNAs were brought into model. Forecast performance was validated in testing datasets. Immune cell infiltration and T-cell activity was weaker in high-risk group compared with that in low-risk counterparts. Innate and adaptive immune cell abundance was inversely proportional to risk score. Compared with low-risk group, patients in high-risk group had lower immune/stromal/ESTIMATE score, lower expression of immune checkpoint molecules, and worse immunotherapy response. **Conclusion**: Six NRG-related lncRNAs were potential targets for future precision therapy of TNBC. Our model was effective in predicting the prognosis of TNBC patients and beneficial for decision-making of immunotherapy.

Keywords: Triple-negative breast cancer; Necroptosis, lncRNA; Risk model; Prognosis; Immune landscape

Abbreviations

BC: Breast Cancer

CTLA-4: Cytotoxic T Lymphocyte-Associated Antigen-4

DC: Dendritic Cell

DEG: Differentially Expressed Genes

ER: Estrogen Receptor

FC: Fold Change

FDR: False Discovery Rate

FPKM: Fragments Per Kilobase of Exon model per Million mapped fragments

GSEA: Gene Set Enrichment Analysis

HCC: Hepatocellular Carcinoma

HDAC: Histone Deacetylase 9

HER-2: Human Epidermal Growth Factor Receptor 2

HR: Hazard Ratio

ICI: Immune Checkpoint Inhibitor

IPS: ImmunoPhenoScore

KEGG: Kyoto Encyclopedia of Genes and Genomes

LASSO: Least Absolute Shrinkage and Selection Operator

lncRNA: Long Non-coding RNA

MLKL: Mixed Lineage Kinase domain-like proteins

NK: Natural Killer

NRG: Necroptosis-Related Gene

NTNBC: Non-Triple-Negative Breast Cancer

PD-1: Programmed Death-1

PLA2G4E: Phospholipase A2 group IVE

PR: Progesterone Receptor

RIPK1/3: Receptor-Interacting serine/Threonine-Protein Kinase 1/3

ROC: Receiver Operating Characteristic

ROS: Reactive Oxygen Species

ssGSEA: Single Sample Gene Set Enrichment Analysis

TCGA: The Cancer Genome Atlas

TCIA: The Cancer Immunome Atlas

TME: Tumor microenvironment

TNBC: Triple-Negative Breast Cancer

Introduction

According to the global cancer statistic GLOBOCAN published in 2020, female breast cancer (BC) was the most common malignancy, with approximately 2.3 million newly diagnosed cases (11.7%). It took the fourth place (6.9%) regarding cause of cancer-specific death of female patients globally [1]. Triple-negative BC (TNBC) is one of four main subtypes of BC. Different from the other three types, TNBC lacks of expression of estrogen and progesterone receptors (ER, PR) as well as the expression of human epidermal growth factor receptor 2 (HER-2). This characteristic makes it the most aggressive and refractory BC subtype, especially in younger patients [2,3]. Traditional endocrine treatment (tamoxifen and aromatase inhibitors) and targeting anti-HER-2 therapy trastuzumab are ineffective in patients with TNBC [4]. Although neoadjuvant systemic therapy was used in early-stage TNBC to improve survival, a series of age-related adverse events occurred, including cognitive damage and premature ovarian failure, severely affecting life quality [5-7]. What's worse, heterogeneity of TNBC with unknown mechanism of carcinogenesis prompts more individualized anticancer treatments [4].

Necroptosis is termed as a kind of caspase-independent, regulated, and programmed cell death [8]. Different from apoptosis, necroptosis is featured as plasma membrane rupture, followed by releasing intracellular components which stimulating the immune system [9]. Necroptosis is associated with pathology of various types of diseases, including non-tumor and tumor diseases. The former part includes cardiovascular, cerebrovascular, neurodegenerative diseases, a series of infectious diseases, and some special types of ischemic morbidities [8, 10-12]. The latter part consists of hematological and solid malignancies [13-17]. Receptor-interacting serine/threonine-protein kinase 1/3 (RIPK1/3) and mixed lineage kinase domain-like proteins (MLKL) are pivotal molecules in the mechanism of necroptosis in cancers [18-19]. *Via* a cascade of signaling pathways involving interferon receptors (IFNR), T cell receptor (TCR), tumor necrosis factor superfamily (TNFSF), Toll-like receptors (TLR), and various types of physicochemical agents, RIPK1 was activated, which is the process of necroptosis induction [18, 20-22]. In tumor biology, necroptosis serves as a double-edged sword. On one hand, it is capable of inhibiting proliferation, aggression, and metastasis of malignancy; on the other hand, it stimulates production of reactive oxygen species (ROS) and maintains tumor microenvironment (TME)[23-25]. Bench studies have found that the function and survival of luminal or non-luminal BC cells could be impacted by

some specific chemical elements which were capable of regulating necroptosis [26-28]. Hence, regulation of necroptosis could be a brand-new approach for anti-TNBC therapy.

Long non-coding RNAs (lncRNAs) are a large family of endogenous RNAs specifically enriched in exosomes and each lncRNA has more than 200 nucleotides [29]. LncRNAs do not code for protein production [30]. LncRNAs in human tissues have been increasingly explored via bioinformatics and second-generation sequencing techniques [31]. In TME, lncRNAs regulate gene expression, affecting variety of biological process of cancer cells including proliferation, differentiation, migration, cell death, invasion and metastasis, and drug resistance [30,32,33]. Previous studies found that lncRNA could also indirectly affect necroptosis by different pathways. In a study from Germany, researchers found that an intergenic lncRNA, Linc00176, exerted a protective function for hepatocellular (HCC) cells by maintaining the capability of proliferation and survival of cancer cells [34]. In a non-tumor model, scientists have shown that a lncRNA called necrosis-related factor (NRF) was capable of targeting RIPK1/RIPK3 and miR-873 to control necroptosis. miR-873 inhibited necrotic death of cardiomyocytes via inhibiting protein production of RIPK1/RIPK3 [35]. Nevertheless, whether lncRNAs contribute to TNBC invasion and proliferation is still unclear. Further intense investigation of necroptosis-related lncRNAs is necessary for more precise and individualized management for TNBC. In this study, we aim to explore remarkable necroptosis-related genes (NRGs) of TNBC as well as related lncRNAs. Subsequent risk model was built based on these genes to predict prognosis of BC patients.

Materials and methods

Data downloading and pre-processing

Transcriptome RNA-seq datasets [HTseq-Counts and Fragments Per Kilobase of exon model per Million mapped fragments (FPKM)] of female BC were downloaded from The Cancer Genome Atlas (TCGA, https://portal.gdc.cancer.gov/). Corresponding clinical data were acquired from cbioportal (https://www.cbioportal.org/). Gene expression matrices from HTseq-Count FPKM files were created via the strawberry perl algorithm (perl 5, version 30). The Count matrix was used to filter the differentially expressed coding genes between TNBC and NTNBC samples, while the FPKM matrix was used for identification of DEG-correlated lncRNAs as well as other analysis. After excluding 12 male samples, 112 normal samples, and 183 samples with unknown state of BC immunohistochemistry (ER, PR, HER-2), 901 samples were used for DEG analysis. For prognosis and immune response studies, 779 female BC samples without unclear clinicopathological information (age, race, staging, subtype, surgery, survival time, etc) were finally included (Supplementary Figure 1).

Source of NRGs and identification of NRG-related lncRNA

226 NRGs were collected from: 1) M24779.gmt in GO gene sets downloaded from the website of Gene Set Enrichment Analysis (GSEA) (http://www.gsea-msigdb.org/gsea/msigdb/search.jsp)[36-38]; 2) map04217 from Kyoto Encyclopedia of Genes and Genomes (KEGG) pathway (https://www.genome.jp/dbget-bin/get_linkdb?-t+orthology+path:map04217); 3) previous literature [39]. DEG analysis was conducted by R package "edgeR" with the filter criterion of log2 fold change (FC) | >1, false discovery rate (FDR) <0.05, and adjusted p value <0.05. After DEG analysis, NRGs with significantly different expression were acquired. For lncRNA data, GENCODE annotation file was used to collect all lncRNAs from the transcriptome matrix via the strawberry perl algorithm. Then correlation analysis was conducted between necroptosis-related DEGs and lncRNAs using Pearson's correlation algorithm. 154 lncRNAs with correlation >0.4 and p value <0.001 was identified as necroptosis-related lncRNAs. The above screening process was performed via R package "limma".

Prognosis-associated lncRNAs and establishment of a prognostic prediction model

We merged the clinical data and data of expression of necroptosis-related lncRNAs. The merged file had 864 BC samples. Then we divided these samples into two subgroups with 1:1 ratio. One group was called as "training set" and the other one was called as "testing set". In the training set, univariate Cox regression analysis was preliminarily performed to select prognostic-classified lncRNAs with p value <0.1. Least absolute shrinkage and selection operator (LASSO) regression was subsequently performed to filter prognosis-related lncRNAs with 10-fold cross-validation and 1,000-cycle running as well as a p value of 0.05. Then the prediction model was created by multivariate Cox regression analysis in the training set, and then the model was used to predict the risk of each sample in the training and testing set, respectively. The risk score was calculated by the following formula:

Risk score= $\sum_{k=1}^{n} expr\left(lncRNA^{k}\right) * coef\left(lncRNA^{k}\right)$ (1), in which "expr" stands for the expression of lncRNA in each sample while "coef" stands for the coefficient of lncRNAs correlated with survival. Median risk scores in both sets were calculated to evaluate the risk of each sample as either "high" or "low" risk so that the samples would be stratified into low-risk or high-risk groups. Clinicopathological variables including age, race, subtype, and type of surgery were evaluated by multi-Cox regression analysis to select potential predictors for nomogram preparation. Receiver operating characteristic (ROC) curves were created to measure the quality of prediction of model. The above analysis was completed via R packages "survival", "rms", "foreign", "caret", "glmnet", "survminer", and "timeROC". Survival analysis between high-

and low- risk groups was conducted with R packages "survival" and "survminer".

Construction of nomogram and calibrated plots

Nomogram was produced according to the results of multivariate Cox regression analysis. Clinicopathological features with p value <0.05 were included in the nomogram. Based on each point derived from every variable, a total point of each sample could be acquired so that the nomogram could predict 1-year, 3-year, 5-year, and 10-year survival rates. To evaluate the predictive accuracy of the nomogram, 1-year, 3-year, 5-year, and 10-year calibrated plots were illustrated. R packages "rms", "survival", and "foreign" were used in this analysis.

GSEA analysis

According to high-risk and low-risk group in all 864 available BC samples, we classified differentially expressed KEGG pathways into different groups through Gene Set Enrichment Analysis software (GSEA, version 4.1.0, Broad Institute, Inc., Massachusetts Institute of Technology, and Regents of the University of California, USA)[36-40]. Amongst, 91 biological functions and pathways were active in high-risk group, while 87 biological functions and pathways were active in low-risk group. We selected each five significantly enriched biological process and pathways in high-and low-risk group, respectively, based on p value< 0.05 and FDR< 0.25.

Comparison of immune landscape between high-risk and low-risk groups

For correlation between immune cell infiltration and risk score, we firstly downloaded the immune cell infiltration file from TIMER (http://timer.cistrome.org/) [41-43]. This file includes data of tumor-infiltrating immune cells derived from several types of algorithms (XCELL, TIMER, QUANTISEQ, MCPCOUNTER, EPIC, and Cibersort). Using Spearman correlation test, we calculated correlations of different immune cells with different risk scores, which is illustrated in a bubble chart. Immune-cell infiltration was furtherly assessed by single sample gene set enrichment analysis (ssGSEA) and major immune functions were also evaluated between high-risk and low-risk group. ssGSEA and its visualization was performed with the help of R packages "GSVA", "limma", "GSEABase", "ggpubr", and "reshape2".

TME and immunotherapy response between high-risk and low-risk groups

Based on Estimate algorithm, we evaluated the TME status by calculating immune score, stromal score, and ESTIMATE score (immune score + stromal score). Then we compared these scores between high- and low-risk groups [44]. We collected immune checkpoint molecules from ImmPort website (https://www.immport.org/shared/genelists) and extracted their expression levels from FPKM file [45,46]. Then we compared their expressions between patients with different risk levels. Finally, potential efficacy of immunotherapy [anti- programmed death-1 (PD-1) and anti-cytotoxic T lymphocyte-associated antigen-4 (CTLA-4) monoclonal antibodies] in the two groups were evaluated by using data of immunophenoscore (IPS) from the Cancer Immunome Atlas (TCIA, https://tcia.at/home)[47,48]. IPS is an effective predictor of treatment response to immune checkpoint inhibitor (ICI), anti-CTLA-4/anti-PD-1 antibodies. Its calculation is based on four categories of immunogenicity: expression of effector cells ($CD4^+$ T cells, activated $CD8^+$ T cells, and memory CD4/$CD8^+$ T cells), immunosuppressive cells (regulatory T cells and myeloid-derived suppressive cells), major histocompatibility complex (MHC) molecules, and immunomodulators. Previous results showed that IPS was associated with several kinds of solid malignancies including BC [49].

The complete process of statistical analysis was performed by R software 4.0.4 (R Foundation for Statistical Computing, Vienna, Austria).

Results

DEG analysis of necroptosis-related genes and associated lncRNAs

According to the clinical data from cbioportal, we divided the 901 female BC samples into two groups: NTNBC group (N=786) and TNBC group (N=115). For 226 NRGs, 203 genes were finally included in analysis. Seven NRGs were DEGs, among which two genes [phospholipase A2 group IVE *(PLA2G4E)*, histone deacetylase 9 (*HDAC9*)] were upregulated in TNBC samples whereas the other 5 genes (H2AC 4/12/14/20/21) were downregulated in TNBC samples (Table 1). Through correlation analysis, 153 NRG-related lncRNAs were obtained, which is illustrated as a network plot (Figure 1).

	Log_2FC	logCPM	P-Value	FDR
HDAC9	1.354052	9.650208	3.02×10-22	5.58×10-20
H2AC14	-1.74302	3.956773	4.07×10-07	3.77×10-05
H2AC20	-1.05981	6.545059	2.52×10-06	0.000117
H2AC4	-1.56114	3.309498	1.03×10-05	0.000382
H2AC12	-1.4443	3.925882	3.21×10-05	0.000988
H2AC21	-1.22542	4.482318	0.000315	0.008333
PLA2G4E	1.026152	4.51469	0.000374	0.008647

Table 1: List of differentially expressed necroptosis-related genes; CPM counts per million, FC fold change, FDR false discovery rate, HDAC Histone deacetylase 9, PLA2G4E Phospholipase A2 group IVE.

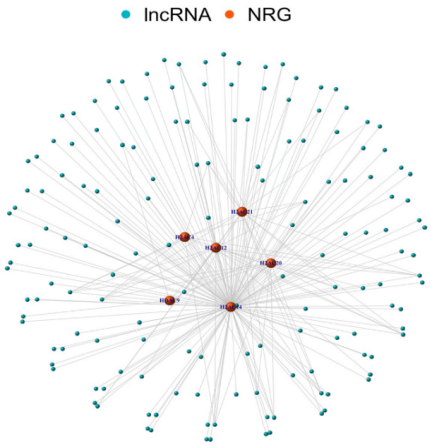

Figure 1: Network between differentially expressed NRG and NRG-related lncRNA; lncRNA long non-coding RNA, NRG necroptosis-related gene. Lines between two nodes indicate significant correlations between lncRNA and NRG.

Construction of a prognostic prediction model for risk assessment

The complete process of model construction was conducted in the training set (N=432). Twelve NRG-related lncRNAs were significantly associated with prognosis according to univariate Cox regression analysis (Figure 2A). Seven of them were indicative of poor prognosis while the other five suggested a protective element of prognosis. Ten lncRNAs with significantly association with prognosis were acquired by LASSO analysis (Figure 2B-2C). Ultimate six prognosis-related lncRNAs were resulted from multivariate Cox analysis, in which expression of three lncRNAs [Z68871.1, SPRY4-AS1, AC011247.1, hazard ratio (HR)>1] were high-risk elements for prognosis and the other three played a protective role in prognosis (COL4A2-AS1, CCDC144NL-AS1, ADAMTS9-AS2, HR<1) (Figure 2D). Based on the results of multi-Cox regression, we obtained a risk score of each sample in the training set using the formula below:

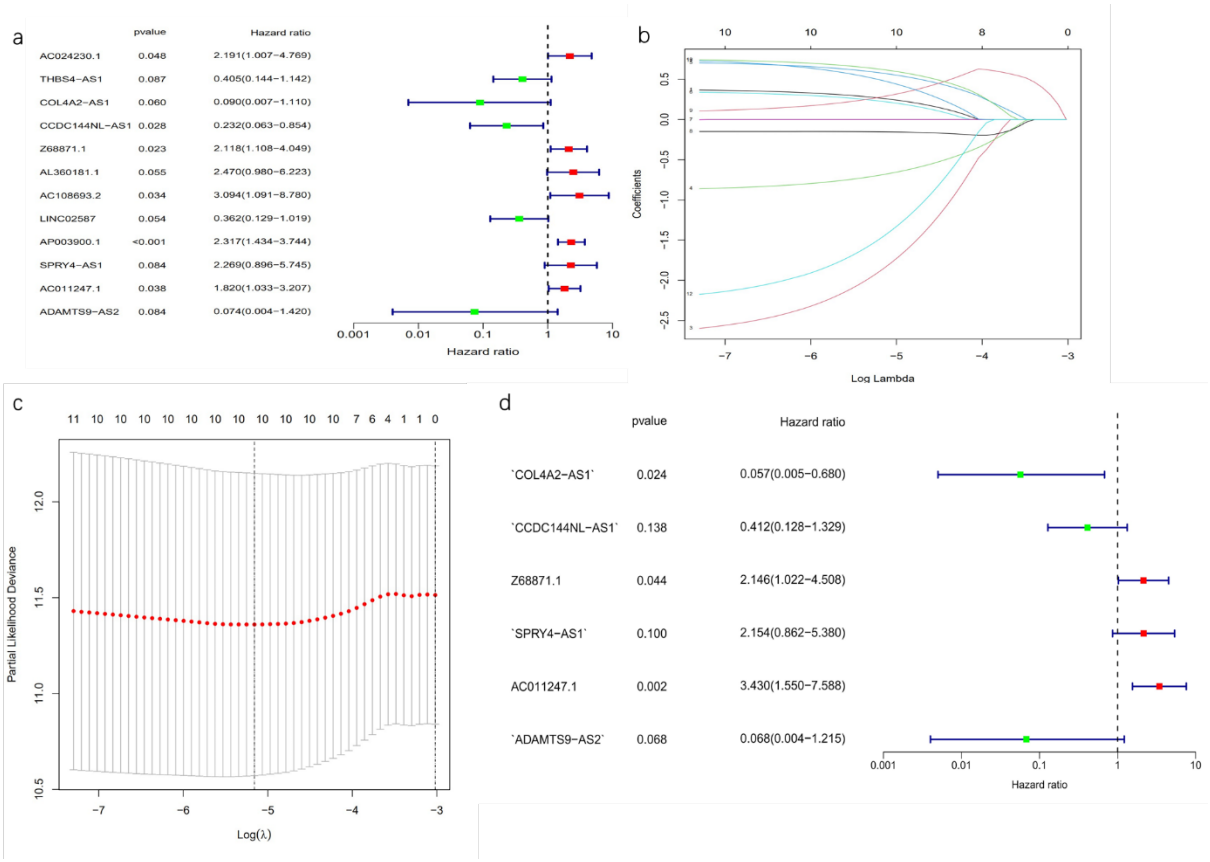

Figure 2: Construction of a risk model with prognostic necroptosis-related lncRNAs. (a) Forest plot of univariate Cox regression analysis of prognosis-related lncRNAs; (b) 10-fold cross-validation for selection of variables in the LASSO model; (c) The LASSO coefficient profile of ten survival-associated lncRNAs; (d) Forest plot of multivariate Cox regression analysis of six prognosis-related lncRNAs; LASSO least absolute shrinkage and selection operator, lncRNA long non-coding RNA.

Risk score= expr (COL4A2-AS1) * (-2.872) + expr (CCDC144NL-AS1) * (-0.887) + expr (ADAMTS9-AS2) * (-2.694) + expr (AC011247.1) * (1.232) + expr (SPRY4-AS1) * (0.767) + expr (Z68871.1) * (0.763). (2)

Then we used this formula to calculate the risk score of samples in the testing set. In both groups, samples were stratified into high-risk and low-risk levels according to the median risk score (Supplementary Figure 2A-C). Survival analysis suggested that patients in high-risk group had a significant poorer overall survival than those of low-risk group, no matter in the training or testing set (Figure 3A-3C, Supplementary Figure 2D-2F). Heatmap reaffirmed the results that lncRNAs Z68871.1, SPRY4-AS1, and AC011247.1 were highly expressed in high-risk groups while the other three lncRNAs COL4A2-AS1, CCDC144NL-AS1, and ADAMTS9-AS2 were highly expressed in low-risk groups, no matter in training, testing or the complete datasets, suggesting their prognostic meaning (Supplementary Figure 2G-2I). The association of clinicopathological factors other than risk scores with overall survival was analyzed and the results showed that risk score together with age, tumor stage, subtype, and type of surgery were independent risk factors of overall survival. Multi-Cox regression analysis demonstrated that older age, higher staging of BC, TNBC, and more invasive operation of BC were indicative of a poorer prognosis (Figure 3D-3E).

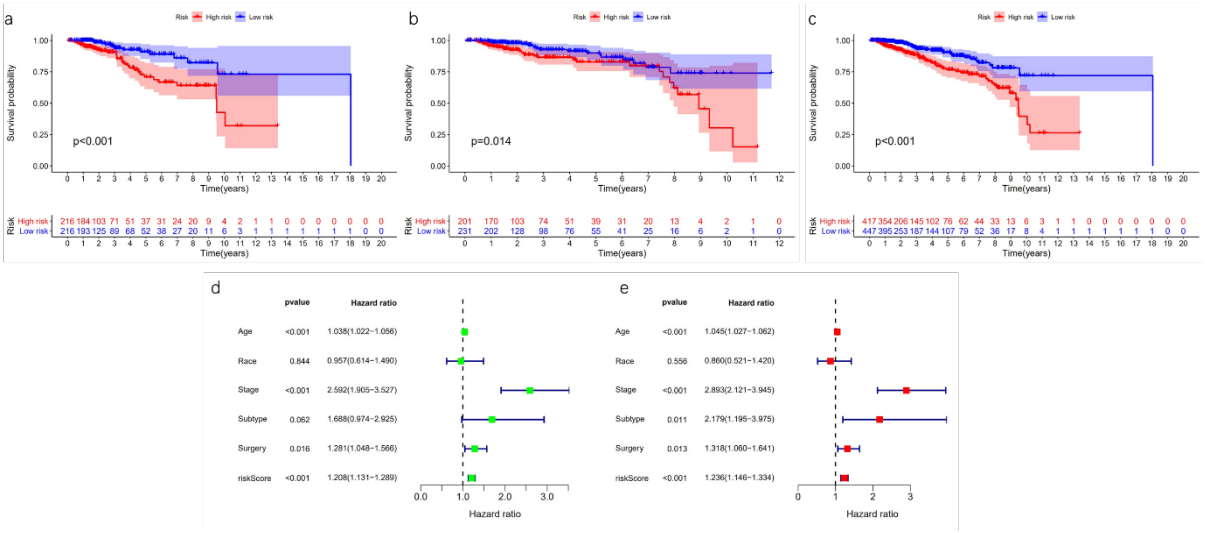

Figure 3: Prognostic analysis of risk model in different sample sets. (a-c) Kaplan–Meier survival curves of overall survival of breast cancer patients between high- and low-risk group in training, testing, and entire samples sets, respectively; (d-e) Forest plots visualizing independent clinicopathological variables of overall survival in the entire sample set.

ROC curves illustrating the area under curve (AUC) in terms of 1-, 3-, 5- , and 10-year were 0.718, 0.623, 0.670, and 0.720 (Figure 4A). Regarding 10-year ROC curves of the model, the AUC of the variable "risk score" was larger than any other clinicopathological variables (AUC=0.720), illustrating a relatively powerful predictive capability (Figure 4B). The HR of risk score in uni- and multivariate Cox model was 1.208 and 1.236, respectively (both p value<0.0001).

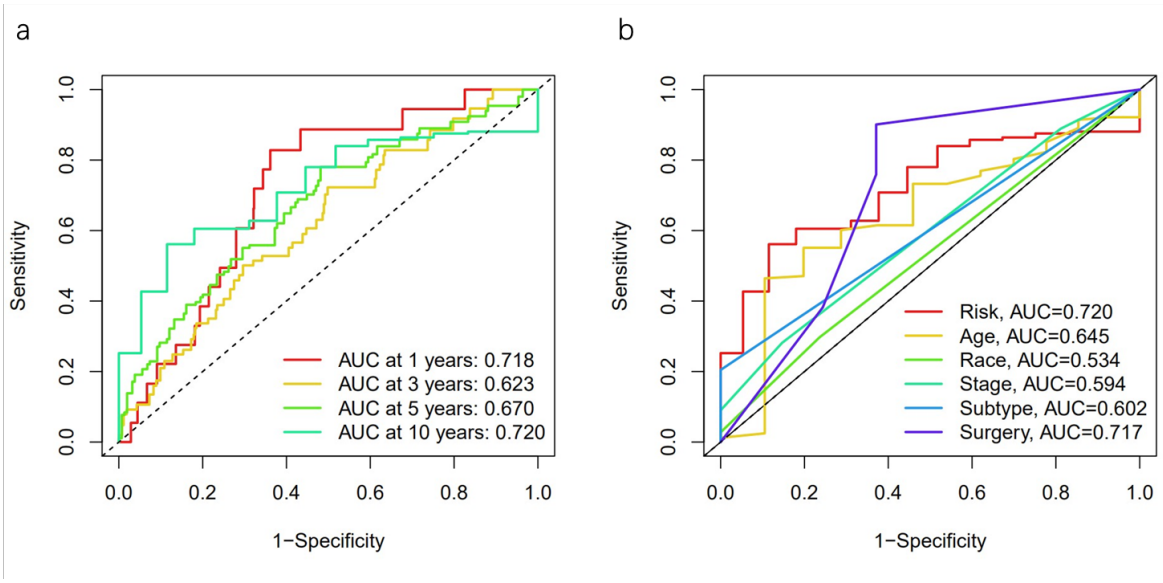

Figure 4: ROC curves of the risk model in different comparisons. (a) 1-, 3-, 5-, 10-year ROC curves of the model in complete sample set; (b) 10-year ROC curves for different clinicopathological variables; AUC area under curve, ROC receiver operating characteristic.

Nomogram construction and calibration plot assessment

Based on the results of the multivariate Cox model for survival analysis, we brought variables "risk score", "age", "stage", "subtype", and "type of surgery" into the nomogram, a visualization tool for prediction of 1-year, 3-year, 5-year, and 10-year survival rate (Figure 5A). Calibration plot demonstrates that the nomogram exhibited an excellent concordance with prediction (Figure 5B).

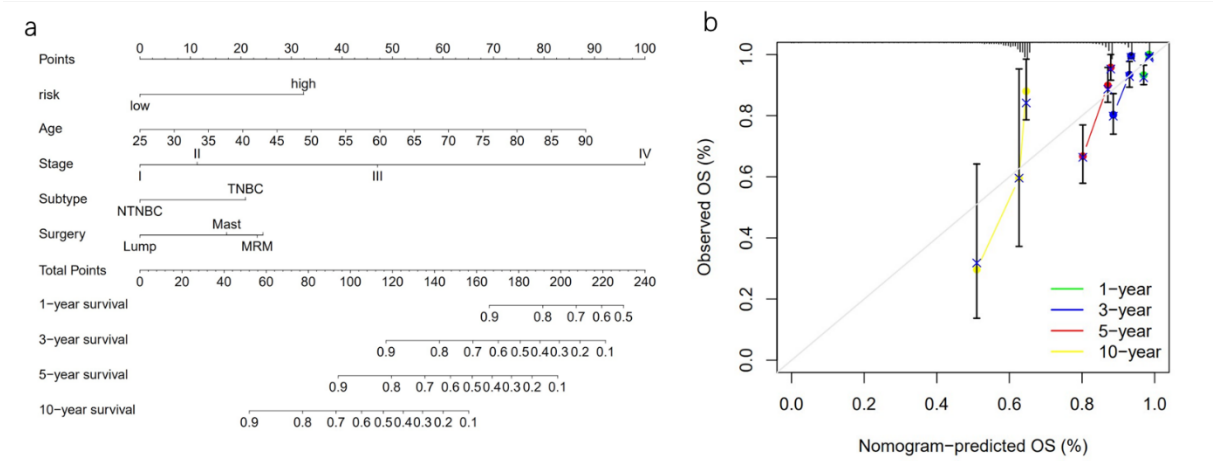

Figure 5: Nomogram of the model and the calibration curves for model validation. (a) Nomogram of the model for prediction of 1-, 3-, 5-, and 10-year overall survival; (b) calibration curves validating the prediction of 1-, 3-, 5-, and 10-year overall survival; Lump lumpectomy, Mast simple mastectomy, MRM modified radical mastectomy, NTNBC non-triple-negative breast cancer, OS overall survival, TNBC triple-negative breast cancer.

Biological pathway analysis

Through GSEA analysis, we summarized different KEGG biological process and pathways in high-risk (N=417) and low-risk (N=447) groups. Each five of significantly enriched biological functions and/or pathways were collected from high- and low-risk groups, respectively. Amongst, high-risk groups included DNA mismatch repair, DNA replication, nucleotide excision repair, RNA degradation, and cell cycle regulation; low-risk groups included cytokine receptor interaction, calcium signaling pathway, TGF-β signaling pathway, regulation of actin cytoskeleton, and cancer pathway (Figure 6).

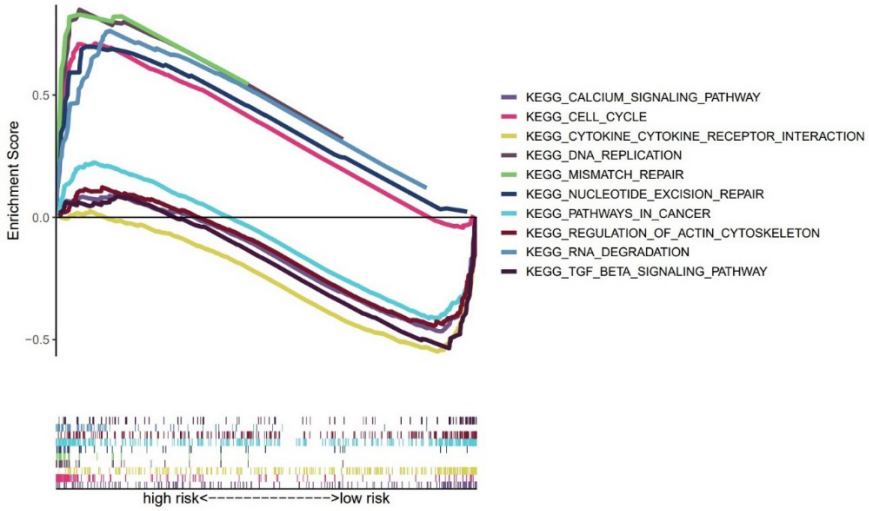

Figure 6: GSEA analysis of the top five KEGG biological pathways in high- and low-risk groups, respectively. GSEA Gene Set Enrichment Analysis, KEGG, Kyoto Encyclopedia of Genes and Genomes.

Comparison of immune signature, TME between high- and low-risk groups

Through ssGSEA, significant discrepancy of immune cell abundance could be found between high- and low-risk groups, especially cytotoxic T cells, B cells, natural killer cells (NK cells), dendritic cells (DCs), and neutrophils. Low-risk group had a higher immune cell infiltration than its counterpart (Figure 7A), which is in line with the result of the activity of major immune functions (cytolytic activity, T-cell costimulation, and interferon response, etc.) between the two groups (Figure 7B).

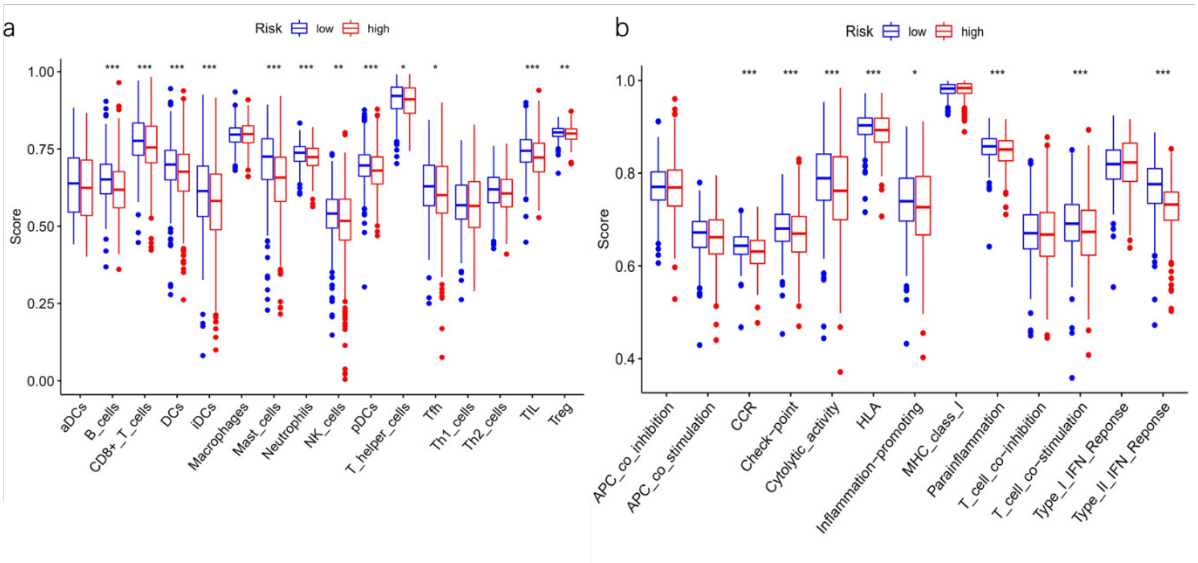

Figure 7: ssGSEA analysis of immune landscapes in high- and low-risk group in the entire sample set. (a) Enrichment level of major immune cells in samples from high- and low-risk groups; (b) Activity level of typical immune functions or pathways between high- and low-risk groups; aDC activated dendritic cell, APC antigen presenting cell, CCR chemokine receptor, DC dendritic cell, HLA human lymphocyte antigen, iDC immature dendritic cell, IFN interferon, MHC major histocompatibility complex, NK cell natural killer cell, pDC plasmacytoid dendritic cell, ssGSEA single sample Gene Set Enrichment Analysis, Tfh follicular helper T cell, Th helper T cell, TIL tumor-infiltrating lymphocyte, Treg regulatory T cell; ***, $p<0.001$; **, $p<0.01$; *, $p<0.05$.

Correlation analysis between immune cell infiltration and risk score was also performed and data were derived from several algorithms (XCELL, TIMER, QUANTISEQ, MCPCOUNTER, EPIC, and CIBERSORT, Figure 8A). Take TIMER algorithm for instance, scatter plots demonstrate that T cells ($CD4^+$, $CD8^+$), B cells, DCs, and neutrophils were all negatively correlated with the risk score which corroborated the results of ssGSEA above (Figure 8B-8F).

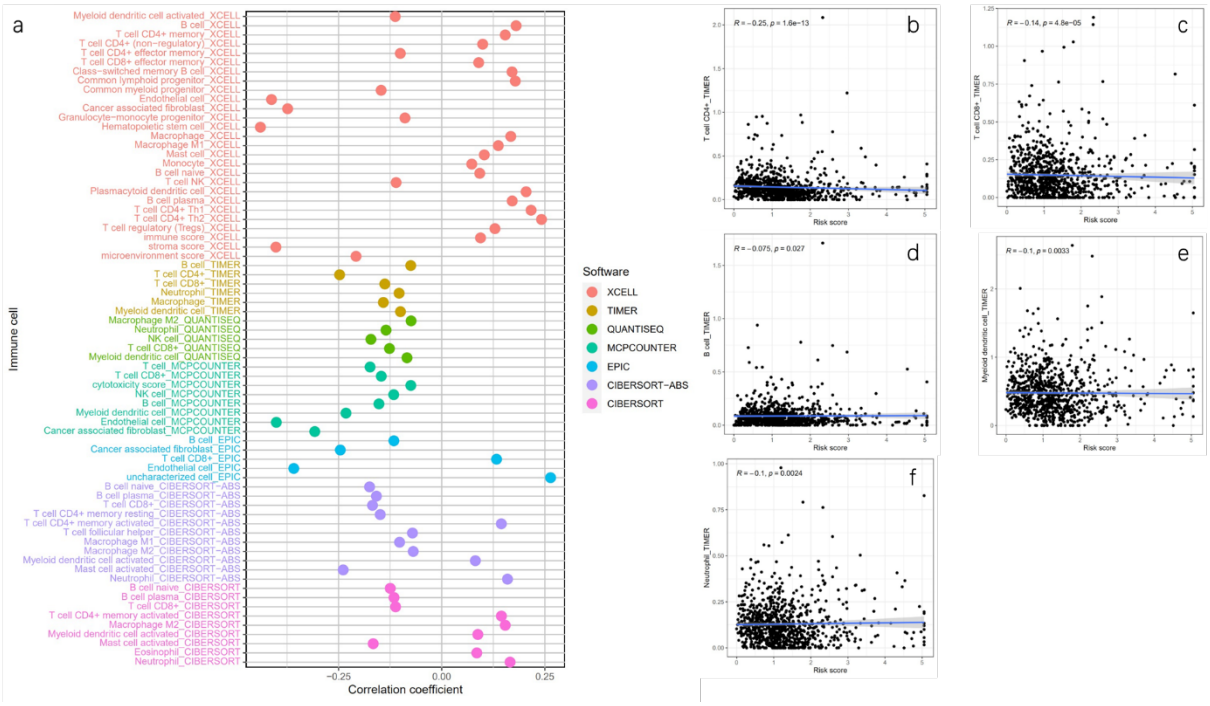

Figure 8: Correlation of major innate and adaptive immune cell infiltration with different risk scores in the entire sample set. (a) Bubble plot demonstrating the correlation between immune cell infiltration with risk score via different various algorithms; (b-f) correlation of infiltration scores of $CD4^+$ T cells (b), $CD8^+$ T cells (c), B cells (d), myeloid Dendritic cells (e), and neutrophils (f) with risk scores.

Furthermore, we calculated immune scores and stromal scores for each BC patients and the boxplots show that patients with higher risk had lower immune/stromal/ESTIMATE scores than patients with lower risk (Figure 9A-9C).

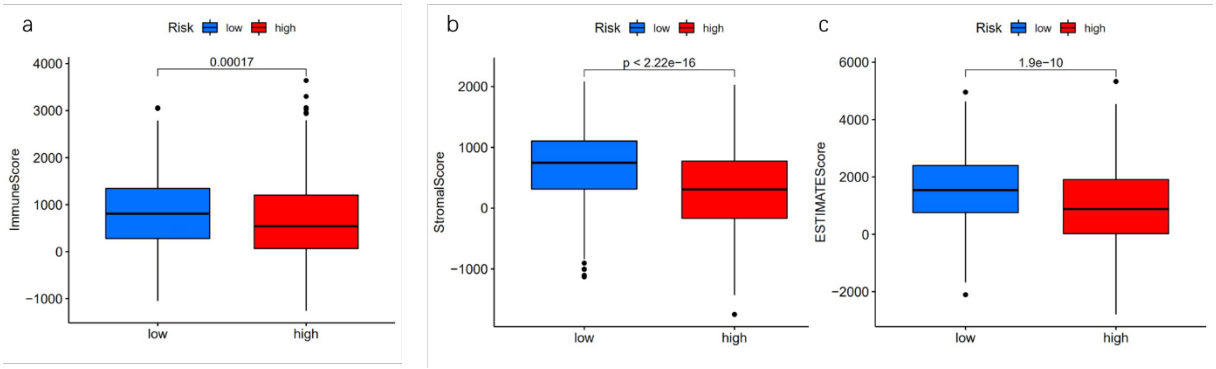

Figure 9: Comparison of tumor microenvironment of samples in entire sample sets between groups with different risk levels. (a) Comparison of immune cell infiltration between high- and low-risk group; (b) Comparison of stromal cell infiltration between high- and low-risk group; (c) Comparison of ESTIMATE score between high- and low-risk group. ESTIMATE score is the sum of the immune and stromal score.

Comparison of immune checkpoint molecules and potential immunotherapy response between different risk levels

47 immune checkpoint molecules were collected and the expression of these genes were extracted from the original FPKM file of female BC samples. We compared the expression level of these genes between high- and low-risk group, which is demonstrated in Figure 10.

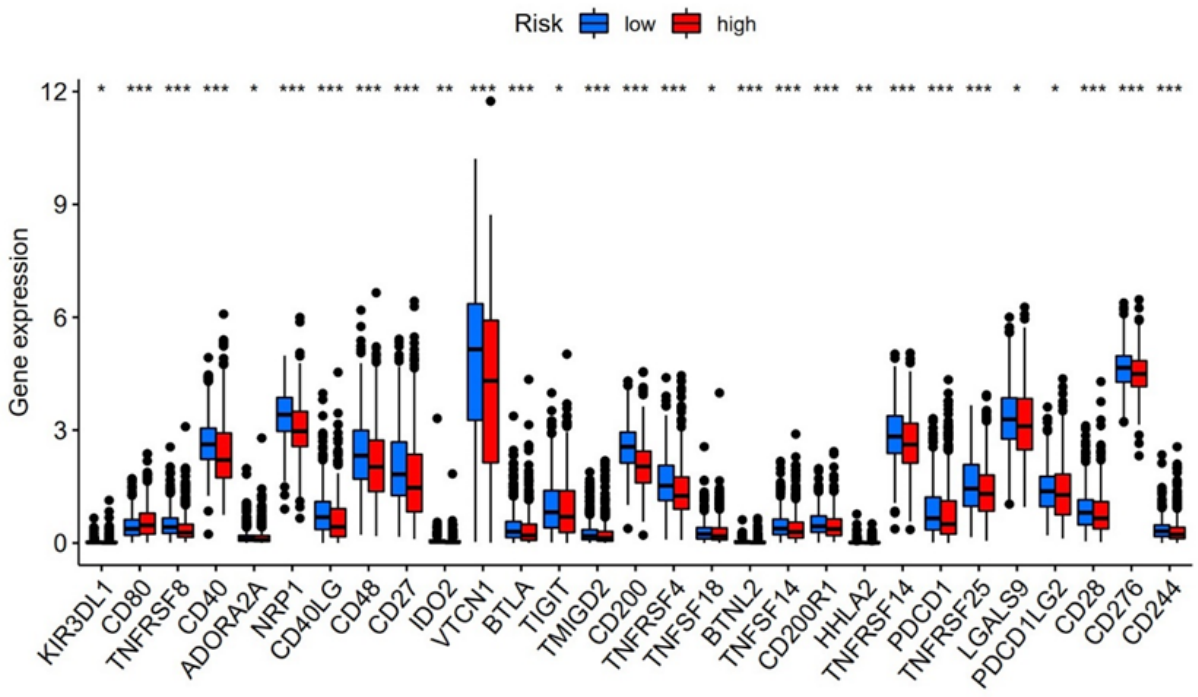

Figure 10: Expression of typical types of immune checkpoint molecules between high- and low-risk groups in the entire sample set; ***, $p<0.001$; **, $p<0.01$; *, $p<0.05$.

Results showed that expression of genes in low-risk group were higher than that of high-risk group except CD80. IPS of patients in high/low-risk groups were obtained. Score 2 (IPS-PD-1/PD-L1/PD-L2 blocker), score 3 (IPS-CTLA-4 blocker), and score 4 (IPS-PD-1/PD-L1/PD-L2 and CTLA-4 blocker) in low-risk group were significantly higher than those in high-risk group (Figure 11A-11D), suggesting a better expected response of ICIs (anti-PD-1/anti-CTLA-4 monoclonal antibodies) in the former group. The results were consistent with the counterpart of immune landscape and TME mentioned in the previous section.

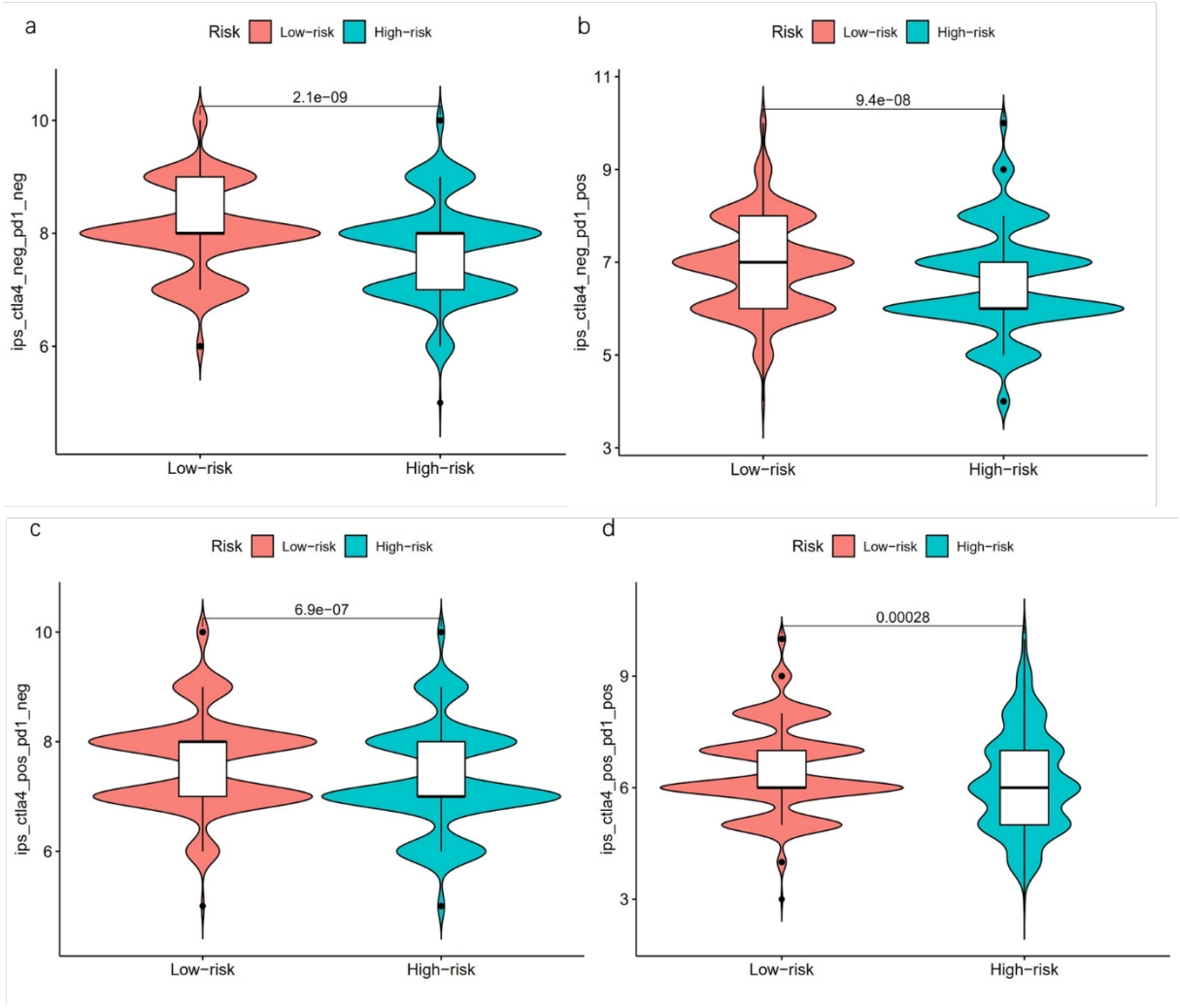

Figure 11: Comparison of IPS of anti-PD-1 and anti-CTLA-4 monoclonal antibody between high- and low-risk group in the entire sample set. (a) pure IPS-1 score between two groups; (b) IPS-1/PD-1 blocker score between two groups; (c) IPS-1/CTLA-4 blocker score between two groups; (d) IPS-1/PD-1/CTLA-4 score between two groups; CTLA-4 cytotoxic T lymphocyte-associated antigen-4, IPS immunophenoscore, neg negative, pos positive, PD-1 programmed death-1.

Discussion

In our study, seven DEGs were found related to necroptosis between NTNBC group and TNBC group. Amongst, *PLA2G4E* and *HDAC9* were upregulated in TNBC samples while H2AC 4/12/14/20 were downregulated in TNBC samples. *PLA2G4E* belongs to the cytosolic phospholipase A2 group IV family. This group of genes regulate membrane tubule-mediated transport. Proteins produced by this gene get involved in recreating tubules to move specific cargo molecules back to cell surface (see details in https://www.ncbi.nlm.nih.gov/gene/123745). Previous studies have found that PLA2G4E was related to necroptosis. Inhibition of *PLA2G4E* by *microRNA Mir504-5p* reduced necroptosis of skin and prolonged survival of skin cells [50]. Previous studies have found that inactivated function of *RIPK1, RIPK3,* and *MLKL*, especially by the necroptosis inhibitor *Nec‐1*, protected neurons from being damaged, degenerated, and keeping the viability of neural cells in these neurodegenerative diseases [51-55]. In an animal model of Alzheimer´s disease, *PLA2G4E* served as a protective role for the survival of cerebral tissue. Overexpression of *PLA2G4E* could resume memory and cognition, indicating a potential role in treatment of neural degenerative disease [56]. It is worthwhile to further explore relationship between this gene and necroptosis in neurodegenerative diseases. *HDAC9* is a member of the class IIa family of histone deacetylases. This gene family get involved

in gene silencing by modifying chromatin into a transcriptionally repressed conformation. *HDAC9* are expressed in many human tissues and organs, especially in brain and skeletal muscles [57,58]. *HDAC9* negatively regulates muscle differentiation by interacting with myocyte enhancer factor (*MEF2*) and inhibiting its transcriptional activity [59]. Similar to *PLA2G4E, HDAC9* also plays a protective role in the nervous system. One study has found that reduced expression of *HDAC9* caused death of neural cells [60]. *HDAC9* possesses several functions in carcinogenesis as well. It has been found to be upregulated in various types of tumors including BC, hepatocellular carcinoma, pancreatic cancer, osteosarcoma, and hematological malignancies [4, 61-65]. In BC, researchers found that overexpression of *HDAC9* was associated with metastasis and poor prognosis [62]. *HDAC9* upregulated NF-κB expression and its downstream inflammatory pathways, stabilizing TME and leading to recurrence of BC [61]. Another study led by Salgado et.al found that *HDAC9* was overexpressed in TNBC, which was consistent with our results [66]. HDAC contributed to increased invasion and angiogenesis in TNBC tissues *via* VEGF and MAPK3 signaling pathway, which is negatively affected by miR-206. A bench study from China using genome-wide CRISPR screening found that *HDAC9* was a pivotal molecule in regulating paclitaxel-resistance of TNBC. Inhibition of *HDAC9* caused tubulin instability and cell cycle arrest, leading to cancer cell death and increasing the sensitivity to chemotherapy [67]. Other related studies also found that HDAC9 suppressed the expression of Erα and endowed antiestrogen-resistance to BC cells [68]. These results indicated a potential HDAC-targeting therapy in the treatment of TNBC to suppress its aggression and improve the sensitivity of TNBC to systemic therapy. Different from the upregulated genes, the significantly downregulated NRGs in TNBC samples were all H2A clustered genes. Proteins encoded by these genes were all belong to replication-dependent histone H2A family (see https://www.ncbi.nlm.nih.gov/gene/8338). A study led by Su found that H2AC was upregulated in ER-positive BC. Suppression of this replication-dependent histone H2A isotype caused abnormal estrogen signaling and cell cycle arrest of BC [69]. In another study, the authors also furtherly found that H2AC was related to telomeres in human cells and interacted with telomeres protein 1 (POT1) as well as telomere repeat factor 2 (TRF2). Depletion of H2AC would dysfunction the telomere, destabilize chromosome structure, and cause DNA damage [69].

According to the correlation analysis, 153 lncRNAs were significantly associated with six of the seven necroptosis-related DEGs (PLA2G4E did not appear in the network). After univariate Cox regression, LASSO regression, and multivariate Cox regression analysis, final 6 prognosis-related lncRNAs were brought into the risk prediction model, including Z68871.1, SPRY4-AS1, AC011247.1, COL4A2-AS1, CCDC144NL-AS1, and ADAMTS9-AS2. Several bioinformatic studies found that high expression of Z68871.1 and SPRY4-AS1 were correlated with worse OS in solid tumors including BC, HCC, and squamous cell carcinoma [69-73]. High expression of ADAMTS9-AS2 was related to a better treatment response and prognosis in BC [74,75], which was coherent with our results. However, high expression of COL4A2-AS1, CCDC144NL-AS1, and ADAMTS9-AS2 were related to proliferation and worse prognosis of breast, gastric, colorectal cancer, HCC, and lung cancer [76-81]. Given that details about functions and involved pathways are unclear, more intense research should be conducted to explore the role of these lncRNAs in BC.

According to the expression and coefficient of lncRNAs, we constructed the model and measured the risk scores for each sample in the training set and testing set. Samples in both sets were stratified into two subgroups: high-risk group and low-risk group. Survival analysis in both sets were similar that patients in high-risk group had a worse prognosis compared with low-risk counterparts. In addition to risk score, age, tumor stage, subtype, and type of surgery were all independent variables for prognosis. Nomogram including these variables was created to predict 1-, 3-, 5-, and 10-year survival rates for BC patients. Predictive efficacy was testified by ROC curves and calibration plots. Results showed that risk score was the best independent predictor of overall survival.

Based on the results of GSEA, we found that significantly enriched biological pathways were focused on cell cycle, cellular metabolism, and cellular proliferation as well as other special pathways including TGF-β and $Ca2^{+}$ signaling pathways. These are important pathways that necroptosis gets involved in. For instance, tumor-induced endothelial necroptosis triggered tumor cell extravasation and metastasis. TGF-β-activated kinase 1 (TAK1) could inhibit necroptosis of endothelial cells [82,83]. Studies also found that dysfunction or deficiency of TAK1 enhanced the necroptosis in which RIPK3 was upregulated [84]. In another study, scientists found that thymoquinone, an apoptosis-inducing agent with anticancer activity, could also induce necroptosis through elevating cytosolic calcium concentration by endoplasmic reticulum calcium depletion and activation of store-operated calcium entry (SOCE) in lymphoma cell [85].

We compared the immune signatures of BC samples between high-risk and low-risk group. Results showed that low-risk group had higher level of immune cell infiltration, higher immune, and stromal scores, and higher expression level of immune checkpoint molecules. However, expression of CD80 was lower in low-risk group than that in high-risk group. Also named as B7-1, CD80 could not only bind to immune-stimulating signaling molecule CD28 but also combine with immunosuppressive molecule CTLA-4 [86]. As reported, the affinity of CD80 to CTLA-4 was higher than that to CD28, providing its immune-inhibiting feature [87]. A study led by Arutha Kulasinghe found that patients with refractory

TNBC had a higher level of CD80 [88], corroborating with our results. More investigation should be performed to validate this conclusion. Correlation analysis illustrates that the abundance of immune cells (DCs, innate, and adaptive immune cells) was all inversely proportional to the risk score. The above results were consistent with the immunotherapy response prediction that low-risk group had a potentially better response to PD-1 and CTLA-4 monoclonal antibodies. Necroptosis not only directly eliminates tumor cells by promoting cell death, but also indirectly suppress tumor growth and proliferation by inducing immune response in TME [89]. During necroptosis, rupture of the plasma membrane led to outpouring damage associated molecular patterns (DAMPs) into intercellular space, then necroptotic cells recruited immune and inflammatory cells to clear the cell debris and helped tissue repair [89,90]. Animal studies showed that $CD8^+$ T cells and NKT cells played major roles in necroptosis-inducing immune response [91,92]. Necroptotic cells offered tumor antigens and inflammatory stimuli to antigen-presenting cells (APC), which then activated $CD8^+$ T cells by antigen cross-priming [93]. $CD8^+$ T cells exerted antitumor cytotoxic immunity by producing and secreting multiple cytokines. The above biological process was highly dependent on RIP1 and NF-κB signaling [91]. Different from $CD8^+$ T cells, NKT-induced immune responses were RIPK3-dependent, of which downstream signaling mediated by pGAM5 and Drp1 [92]. Counterintuitively, some researchers suggested that inflammation derived from necroptosis was a pro-cancer factor in TME [94]. In the process of carcinogenesis, inflammation could promote tumor cell growth, proliferation, aggressiveness, invasion, and metastasis by providing bioactive molecules [90,95,96]. ROS and other mutagenic chemicals also facilitated evolution of tumor cells by genetic alterations [90]. Given that the above conclusions were controversial, the contribution of immune and inflammatory responses induced by necroptosis in tumor prevention and development needs to be further elucidated.

Despite a comprehensive analysis of necroptosis in TNBC and its relationship with prognosis and immune landscape, some limitations still existed in our study. Firstly, the results were not further validated in basic studies (*in vitro and in vivo*). The biological functions of prognosis-related lncRNAs were needed to be clarified. Secondly, different extents of biases during data processing and case inclusion/exclusion were inevitable because of a retrospective feature of this study. Thirdly, the expression of PD-1 (CD279) and PD-L1 (CD274) were not included in the original transcriptome data file of TCGA-BRCA. Hence, we failed to directly compare the expression level of these two biomarkers between high- and low-risk groups though data of anti- PD-1 and PD-L1 response could be retrieved from TCIA database.

To conclude, seven differentially expressed NRGs were selected between NTNBC and TNBC groups. Six NRG-related lncRNAs were significantly associated with prognosis and were brought into risk model construction. Risk score is an excellent predictor for overall survival of BC and the model was of high predictive quality. Compared with low-risk group, high-risk group has a gloomier prognosis, less abundance immune cell infiltration, and less responsive ICI treatment. The results pave way for further exploration of precision therapy for TNBC.

Acknowledgements

The authors of this manuscript sincerely appreciate the efforts of all researchers who have contributed the data to the public databases of TCGA, cbioportal, TCIA, and TIMER; GSEA software and algorithm of ESTIMATE. The interpretation and reporting of these data are the sole responsibility of the authors.

Statements & Declarations

Funding

This work was supported by CAMS Innovation Fund for Medical Sciences (CIFMS) under Grant [2021-I2M-1-061 and 2021-1-I2M-003 and 2018-I2M-3-001]; CAMS Clinical and Translational Medicine Research Funds under grant [2019XK320006].

Competing Interests

The authors have no relevant financial or non-financial interests to disclose.

Data Availability Statement

The authors confirm that the data supporting the findings of this study are available within the article and its supplementary materials.

Author Contributions

All authors contributed to the study conception and design. Material preparation, data collection, and analysis were performed by Zijun Zhao, Xiayao Diao, and Qing Cao. The first draft of the manuscript was written by Zijun Zhao and Xiayao Diao and all authors commented on previous versions of the manuscript. All authors read and approved the final manuscript.

Reference

1. Sung H, Ferlay J, Siegel RL, Laversanne M, Soerjomataram I, et al. (2021) Global Cancer Statistics 2020: GLOBOCAN Estimates of Incidence and Mortality Worldwide for 36 Cancers in 185 Countries. CA Cancer J Clin 71: 209-249.
2. Carey LA, Perou CM, Livasy CA, Dressler LG, Cowan D, et al. (2006) Race, breast cancer subtypes, and survival in the Carolina Breast Cancer Study. JAMA 295: 2492-2502.
3. Siddharth S, Sharma D (2018) Racial Disparity and Triple-Negative Breast Cancer in African-American Women: A Multifaceted Affair between Obesity, Biology, and Socioeconomic Determinants. Cancers (Basel) 10: 514.

4. de Jong VMT, Wang Y, Ter Hoeve ND, Opdam M, Stathonikos N, et al. (2022) Prognostic Value of Stromal Tumor-Infiltrating Lymphocytes in Young, Node-Negative, Triple-Negative Breast Cancer Patients Who Did Not Receive (neo)Adjuvant Systemic Therapy. J Clin Oncol 40: 2361-2374.

5. EBCTCG (2019) Increasing the dose intensity of chemotherapy by more frequent administration or sequential scheduling: a patient-level meta-analysis of 37 298 women with early breast cancer in 26 randomised trials. Lancet 393: 1440-1452.

6. Poorvu PD, Frazier AL, Feraco AM, Manley PE, Ginsburg ES, et al. (2019) Cancer Treatment-Related Infertility: A Critical Review of the Evidence. JNCI Cancer Spectr 3: pkz008.

7. Menning S, de Ruiter MB, Kieffer JM, van Rentergem JA, Veltman DJ, et al. (2016) Cognitive Impairment in a Subset of Breast Cancer Patients After Systemic Therapy-Results From a Longitudinal Study. J Pain Symptom Manage 52: 560-569.

8. Galluzzi L, Kroemer G (2008) Necroptosis: a specialized pathway of programmed necrosis. Cell 135: 1161-1163.

9. Degterev A, Huang Z, Boyce M, Li Y, Jagtap P, et al. (2005) Chemical inhibitor of nonapoptotic cell death with therapeutic potential for ischemic brain injury. Nat Chem Biol 1: 112-119.

10. Ji X, Wang R, Tang H, Chen H, Bao L, et al. (2019) Necroptosis of osteoblasts was induced by breast cancer cells in vitro. Transl Cancer Res 9: 500-507.

11. Zhang S, Tang MB, Luo HY, Shi CH, Xu YM, et al. (2017) Necroptosis in neurodegenerative diseases: a potential therapeutic target. Cell Death Dis 8: e2905.

12. Orzalli MH, Kagan JC (2017) Apoptosis and Necroptosis as Host Defense Strategies to Prevent Viral Infection. Trends Cell Biol 27: 800-809.

13. Liu P, Xu B, Shen W, H Zhu, W Wu, et al. (2012) Dysregulation of TNFα-induced necroptotic signaling in chronic lymphocytic leukemia: suppression of CYLD gene by LEF1. Leukemia 26:1293-1300.

14. Koo GB, Morgan MJ, Lee DG, Kim WJ, Yoon JH, et al. (2015) Methylation-dependent loss of RIP3 expression in cancer represses programmed necrosis in response to chemotherapeutics. Cell Res 25: 707-725.

15. Moriwaki K, Bertin J, Gough PJ, Orlowski GM, Chan FKM, et al. (2015) Differential roles of RIPK1 and RIPK3 in TNF-induced necroptosis and chemotherapeutic agent-induced cell death. Cell Death Dis. 6: e1636.

16. Fukasawa M, Kimura M, Morita S, Matsubara K, Yamanaka S, et al. (2006) Microarray analysis of promoter methylation in lung cancers. J Hum Genet 51: 368-374.

17. Cerhan JR, Ansell SM, Fredericksen ZS, Kay NE, Liebow M, et al. (2007) Genetic variation in 1253 immune and inflammation genes and risk of non-Hodgkin lymphoma. Blood 110: 4455-4463.

18. Galluzzi L, Kepp O, Chan FK, Guido Kroemer, et al. (2017) Necroptosis: Mechanisms and Relevance to Disease. Annu Rev Pathol 12: 103-130.

19. Quarato G, Guy CS, Grace CR, Llambi F, Nourse A, et al. (2016) Sequential Engagement of Distinct MLKL Phosphatidylinositol-Binding Sites Executes Necroptosis. Mol Cell 61: 589-601.

20. Mishra AP, Salehi B, Sharifi-Rad M, Pezzani P, Kobarfard F, et al. (2018) Programmed Cell Death, from a Cancer Perspective: An Overview. Mol Diagn Ther 22: 281-295.

21. Su Z, Yang Z, Xu Y, Chen Y, Yu Q (2015) Apoptosis, autophagy, necroptosis, and cancer metastasis. Mol Cancer 14: 48.

22. Vanden Berghe T, Linkermann A, Jouan-Lanhouet S, Walczak H, Vandenabeele P (2014) Regulated necrosis: the expanding network of non-apoptotic cell death pathways. Nat Rev Mol Cell Biol 15: 135-147.

23. Tafani M, Sansone L, Limana F, Arcangeli T, De Santis E, et al. (2016) The Interplay of Reactive Oxygen Species, Hypoxia, Inflammation, and Sirtuins in Cancer Initiation and Progression. Oxid Med Cell Longev. 2016: 3907147.

24. Seifert L, Werba G, Tiwari S, Giao Ly NN, Alothman S, et al. (2016) The necrosome promotes pancreatic oncogenesis via CXCL1 and Mincle-induced immune suppression. Nature 532: 245-249.

25. Weinlich R, Oberst A, Beere HM, Green DR, et al. (2017) Necroptosis in development, inflammation and disease. Nat Rev Mol Cell Biol 18:127-136.

26. Wisowski G, Pudełko A, Olczyk K, Paul-Samojedny M, Koźma EM, et al. (2022) Dermatan Sulfate Affects Breast Cancer Cell Function via the Induction of Necroptosis. Cells 11: 173.

27. Shen F, Pan X, Li M, Chen Y, Jiang Y, et al. (2020) Pharmacological Inhibition of Necroptosis Promotes Human Breast Cancer Cell Proliferation and Metastasis. Onco Targets Ther 13: 3165-3176.

28. Chepikova OE, Malin D, Strekalova E, Lukasheva EV, Zamyatnin AA, et al. (2020) Lysine oxidase exposes a dependency on the thioredoxin antioxidant pathway in triple-negative breast cancer cells. Breast Cancer Res Treat 183: 549-564.

29. Zhang Y, Wei YJ, Zhang YF, Liu HW, Zhang YF, et al. (2021) Emerging Functions and Clinical Applications of Exosomal ncRNAs in Ovarian Cancer. Front Oncol 11:765458.

30. Cantile M, Di Bonito M, Tracey De Bellis M, Botti G, et al. (2021) Functional Interaction among lncRNA HOTAIR and MicroRNAs in Cancer and Other Human Diseases. Cancers (Basel) 13: 570.

31. Zhang YF, Shan C, Wang Y, Qian LL, Jia DD, et al. (2020) Cardiovascular toxicity and mechanism of bisphenol A and emerging risk of bisphenol S. Sci Total Environ 723: 137952.

32. Liu Y, Ding W, Yu W, Zhang Y, Ao X, et al. (2021) Long non-coding RNAs: Biogenesis, functions, and clinical significance in gastric cancer. Mol Ther Oncolytics 23: 458-476.

33. Qi Y, Song C, Zhang J, Zhang J, Guo C, et al. (2021) Oncogenic LncRNA CASC9 in Cancer Progression. Curr Pharm Des 27: 575-582.

34. Tran DDH, Kessler C, Niehus SE, Mahnkopf M, Koch A, et al.(2018) Myc target gene, long intergenic noncoding RNA, Linc00176 in hepatocellular carcinoma regulates cell cycle and cell survival by titrating tumor suppressor microRNAs. Oncogene 37: 75-85.

35. Wang K, Liu F, Liu CY, T An , J Zhang , et al. (2016) The long noncoding RNA NRF regulates programmed necrosis and myocardial injury during ischemia and reperfusion by targeting miR-873. Cell Death Differ. 23: 1394-1405.

36. Subramanian A, Tamayo P, Mootha VK, Mukherjee S, L Ebert BL, et al. (2005) Gene set enrichment analysis: a knowledge-based approach for interpreting genome-wide expression profiles. Proc Natl Acad Sci U S A. 102: 15545-15550.

37. Liberzon A, Subramanian A, Pinchback R, Thorvaldsdóttir H, Tamayo

P, et al. (2011) Molecular signatures database (MSigDB) 3.0. Bioinformatics 27: 1739-1740.

38. Liberzon A, Birger C, Thorvaldsdóttir H, Ghandi M, Mesirov JP, et al. (2015)The Molecular Signatures Database (MSigDB) hallmark gene set collection. Cell Syst 1: 417-425.

39. Zhao Z, Liu H, Zhou X, Fang D, Ou X, et al. (2021) Necroptosis-Related lncRNAs: Predicting Prognosis and the Distinction between the Cold and Hot Tumors in Gastric Cancer. J Oncol 2021: 6718443.

40. Mootha VK, Lindgren CM, Eriksson KF, Subramanian A, Sihag S, et al. (2003) PGC-1alpha-responsive genes involved in oxidative phosphorylation are coordinately downregulated in human diabetes. Nat Genet. 34: 267-273.

41. Li T, Fu J, Zeng Z, Cohen D, Li J, et al. (2020) TIMER2.0 for analysis of tumor-infiltrating immune cells. Nucleic Acids Res 48: W509-W514.

42. Li T, Fan J, Wang B, Traugh N, Chen Q, et al. (2017) TIMER: A Web Server for Comprehensive Analysis of Tumor-Infiltrating Immune Cells. Cancer Res 77: e108-e110.

43. Li B, Severson E, Pignon JC, Zhao H, Li T, et al. (2016) Comprehensive analyses of tumor immunity: implications for cancer immunotherapy. Genome Biol 17: 174.

44. Yoshihara K, Shahmoradgoli M, Martínez E, Vegesna R, Kim H, et al. (2013) Inferring tumour purity and stromal and immune cell admixture from expression data. Nat Commun 4: 2612.

45. Chaussabel D, Baldwin N, et al (2014) Democratizing systems immunology with modular transcriptional repertoire analyses. Nat Rev Immunol 14: 271-280.

46. Li S, Rouphael N, Duraisingham S, Romero-Steiner S, Presnell S, et al. (2014) Molecular signatures of antibody responses derived from a systems biology study of five human vaccines. Nat Immunol 15(2):195-204.

47. Van Allen EM, Miao D, Schilling B, Shukla SA, Blank C, et al. (2015) Genomic correlates of response to CTLA-4 blockade in metastatic melanoma. Science 350: 207-211.

48. Hugo W, Zaretsky JM, Sun L, Song C, Moreno BH, et al. (2016) Genomic and Transcriptomic Features of Response to Anti-PD-1 Therapy in Metastatic Melanoma. Cell 165: 35-44.

49. Charoentong P, Finotello F, Angelova M, Mayer C, Efremova M, et al. (2017) Pan-cancer Immunogenomic Analyses Reveal Genotype-Immunophenotype Relationships and Predictors of Response to Checkpoint Blockade. Cell Rep 18: 248-262.

50. Lou J, Wang X, Zhang H, Yu G, Ding J, et al. (2021) Inhibition of PLA2G4E/cPLA2 promotes survival of random skin flaps by alleviating Lysosomal membrane permeabilization-Induced necroptosis. Autophagy 18: 1841-1863.

51. Zhang Y, Li M, Li X, Zhang H, Wang L, et al. (2020) Catalytically inactive RIP1 and RIP3 deficiency protect against acute ischemic stroke by inhibiting necroptosis and neuroinflammation. Cell Death Dis11: 565.

52. Oñate M, Catenaccio A, Salvadores N, Saquel C, Martinez A, et al. (2020) The necroptosis machinery mediates axonal degeneration in a model of Parkinson disease. Cell Death Differ 27: 1169-1185.

53. Ito Y, Ofengeim D, Najafov A, Das S, Saberi S, et al. (2016) RIPK1 mediates axonal degeneration by promoting inflammation and necroptosis in ALS. Science 353: 603-608.

54. Ofengeim D, Ito Y, Najafov A, Zhang Y, Shan B, et al. (2015) Activation of necroptosis in multiple sclerosis. Cell Rep 10: 1836-1849.

55. Iannielli A, Bido S, Folladori L, Segnali A, Cancellieri C, et al. (2018) Pharmacological Inhibition of Necroptosis Protects from Dopaminergic Neuronal Cell Death in Parkinson's Disease Models. Cell Rep 22: 2066-2079.

56. Petrie Pérez-González M, Mendioroz M, Badesso S, Sucunza D, Roldan M, et al. (2020) PLA2G4E, a candidate gene for resilience in Alzheimer´s disease and a new target for dementia treatment. Prog Neurobiol 191: 101818.

57. Petrie K, Guidez F, Howell L, Healy L, Waxman S, et al. (2003) The histone deacetylase 9 gene encodes multiple protein isoforms. J Biol Chem 278: 16059-16072.

58. Zhou X, Marks PA, Rifkind RA, Richon VM (2001) Cloning and characterization of a histone deacetylase, HDAC9. Proc Natl Acad Sci U S A 98: 10572-10577.

59. Haberland M, Arnold MA, McAnally J, Phan D, Kim Y, et al. (2007) Regulation of HDAC9 gene expression by MEF2 establishes a negative-feedback loop in the transcriptional circuitry of muscle differentiation. Mol Cell Biol 27: 518-525.

60. Morrison BE, Majdzadeh N, Zhang X, Lyles A, Bassel-Duby R, et al. (2006) Neuroprotection by histone deacetylase-related protein. Mol Cell Biol 26: 3550-3564.

61. Bera A, Russ E, Manoharan MS, Srinivasan M, Eidelman O, et al. (2020) Proteomic Analysis of Inflammatory Biomarkers Associated With Breast Cancer Recurrence. Mil Med 185: 669-675.

62. Huang Y, Jian W, Zhao J, Wang G (2018) Overexpression of HDAC9 is associated with poor prognosis and tumor progression of breast cancer in Chinese females. Onco Targets Ther 11: 2177-2184.

63. Freese K, Seitz T, Dietrich P, Lee SML, Thasler WE, et al. (2019) Histone Deacetylase Expressions in Hepatocellular Carcinoma and Functional Effects of Histone Deacetylase Inhibitors on Liver Cancer Cells *In Vitro*. Cancers (Basel) 11:1587.

64. Li H, Li X, Lin H, Gong J (2020) High HDAC9 is associated with poor prognosis and promotes malignant progression in pancreatic ductal adenocarcinoma. Mol Med Rep 21: 822-832.

65. Zhao YX, Wang YS, Cai QQ, Wang JQ, Yao WT (2015) Up-regulation of HDAC9 promotes cell proliferation through suppressing p53 transcription in osteosarcoma. Int J Clin Exp Med 8: 11818-11823.

66. Salgado E, Bian X, Feng A, Shim H, Liang Z (2018) HDAC9 overexpression confers invasive and angiogenic potential to triple negative breast cancer cells via modulating microRNA-206. Biochem Biophys Res Commun 503: 1087-1091.

67. Lian B, Pei YC, Jiang YZ, Xue MZ, Li DQ, et al. (2020) Truncated HDAC9 identified by integrated genome-wide screen as the key modulator for paclitaxel resistance in triple-negative breast cancer. Theranostics 10: 11092-11109.

68. Linares A, Assou S, Lapierre M, Thouennon E, Duraffourd C, et al. (2019) Increased expression of the HDAC9 gene is associated with antiestrogen resistance of breast cancers. Mol Oncol 13: 1534-1547.

69. Su CH, Tzeng TY, Cheng C (2014) An H2A histone isotype regulates estrogen receptor target genes by mediating enhancer-promoter-3'-UTR interactions in breast cancer cells. Nucleic Acids Res 42: 3073-3088.

70. Li X, Jin F, Li Y (2021) A novel autophagy-related lncRNA prognostic risk model for breast cancer. J Cell Mol Med 25: 4-14.

71. Li X, Li Y, Yu X, Jin F (2020) Identification and validation of stemness-related lncRNA prognostic signature for breast cancer. J Transl Med 18: 331.

72. Ye M, Wang S, Qie JB, Sub PL (2021) SPRY4-AS1, A Novel Enhancer RNA, Is a Potential Novel Prognostic Biomarker and Therapeutic Target for Hepatocellular Carcinoma. Front Oncol 11: 765484.

73. Gong S, Xu M, Zhang Y, Shan Y, Zhang H (2020) The Prognostic Signature and Potential Target Genes of Six Long Non-coding RNA in Laryngeal Squamous Cell Carcinoma. Front Genet 11: 413.

74. Ni K, Huang Z, Zhu Y, Xue D, Jin Q, et al. (2021) The lncRNA ADAMTS9-AS2 Regulates RPL22 to Modulate TNBC Progression via Controlling the TGF-β Signaling Pathway. Front Oncol 11: 654472.

75. Shi YF, Lu H, Wang HB (2019) Downregulated lncRNA ADAMTS9-AS2 in breast cancer enhances tamoxifen resistance by activating microRNA-130a-5p. Eur Rev Med Pharmacol Sci 23: 1563-1573.

76. Yu Z, Wang Y, Deng J, Liu D, Zhang L, et al. (2021) Long non-coding RNA COL4A2-AS1 facilitates cell proliferation and glycolysis of colorectal cancer cells via miR-20b-5p/hypoxia inducible factor 1 alpha subunit axis. Bioengineered 12: 6251-6263.

77. Yao Y, Zhang T, Qi L, Zhou C , Wei J, et al. (2019) Integrated analysis of co-expression and ceRNA network identifies five lncRNAs as prognostic markers for breast cancer. J Cell Mol Med 23: 8410-8419.

78. Zhang Y, Peng C, Li J, Zhang D, Zhang C, et al. (2022) Long non-coding RNA CCDC144NL-AS1 promotes cell proliferation by regulating the miR-363-3p/GALNT7 axis in colorectal cancer. J Cancer 13: 752-763.

79. Sheng W, Zhou W, Cao Y, Zhong Y, et al. (2021) Revealing the Role of lncRNA CCDC144NL-AS1 and LINC01614 in Gastric Cancer via Integrative Bioinformatics Analysis and Experimental Validation. Front Oncol11: 769563.

80. Zhang L, Chi B, Chai J, Qin L, Zhang G, et al. (2021) LncRNA CCDC144NL-AS1 Serves as a Prognosis Biomarker for Non-small Cell Lung Cancer and Promotes Cellular Function by Targeting miR-490-3p. Mol Biotechnol 63: 933-940.

81. Zhang Y, Zhang H, Wu S (2021) LncRNA-CCDC144NL-AS1 Promotes the Development of Hepatocellular Carcinoma by Inducing WDR5 Expression via Sponging miR-940. J Hepatocell Carcinoma 8: 333-348.

82. Guo X, Yin H, Chen Y, Li L, Li J, et al. (2016) TAK1 regulates caspase 8 activation and necroptotic signaling via multiple cell death checkpoints. Cell Death Dis 7: e2381.

83. Malireddi RKS, Gurung P, Mavuluri J, Krishna Dasari TK, Klco JM, et al. (2018) TAK1 restricts spontaneous NLRP3 activation and cell death to control myeloid proliferation. J Exp Med 215: 1023-1034.

84. Yang L, Joseph S, Sun T, Hoffmann J, Thevissen S, et al. (2019) TAK1 regulates endothelial cell necroptosis and tumor metastasis. Cell Death Differ 26: 1987-1997.

85. Berehab M, Rouas R, Akl H, Duvillier H, Journe F, et al. (2021) Apoptotic and Non-Apoptotic Modalities of Thymoquinone-Induced Lymphoma Cell Death: Highlight of the Role of Cytosolic Calcium and Necroptosis. Cancers (Basel) 13 :3579.

86. Qureshi OS, Zheng Y, Nakamura K, Attridge K, Manzotti C, et al. (2011) Trans-endocytosis of CD80 and CD86: a molecular basis for the cell-extrinsic function of CTLA-4. Science 332: 600-603.

87. Pentcheva-Hoang T, Egen JG, Wojnoonski K , Allison JP, et al. (2004) B7-1 and B7-2 selectively recruit CTLA-4 and CD28 to the immunological synapse. Immunity 21: 401-413.

88. Kulasinghe A, Monkman J, Shah ET, Matigian N, Adams MN, et al. (2021) Spatial Profiling Identifies Prognostic Features of Response to Adjuvant Therapy in Triple Negative Breast Cancer (TNBC). Front Oncol 11: 798296.

89. Pasparakis M, Vandenabeele P (2015) Necroptosis and its role in inflammation. Nature 517: 311-320.

90. Grivennikov SI, Greten FR, Karin M (2010) Immunity, inflammation, and cancer. Cell 140: 883-899.

91. Yatim N, Jusforgues-Saklani H, Orozco S, Schulz O , da Silva RB, et al. (2015) RIPK1 and NF-κB signaling in dying cells determines cross-priming of CD8 T cells. Science 350: 328-334.

92. Kang YJ, Bang BR, Han KH, Hong L, Shim EJ, et al. (2015) Regulation of NKT cell-mediated immune responses to tumours and liver inflammation by mitochondrial PGAM5-Drp1 signalling. Nat Commun 6: 8371.

93. Sancho D, Joffre OP, Keller AM, Rogers NC, Martínez D, et al. (2009) Identification of a dendritic cell receptor that couples sensing of necrosis to immunity. Nature 458: 899-903.

94. Hanahan D, Weinberg RA (2011) Hallmarks of cancer: the next generation. Cell 144: 646-674.

95. Mantovani A, Allavena P, Sica A, Frances Balkwill (2008) Cancer-related inflammation. Nature. 454: 436-444.

96. Qian BZ, Pollard JW (2010) Macrophage diversity enhances tumor progression and metastasis. Cell. 141: 39-51.

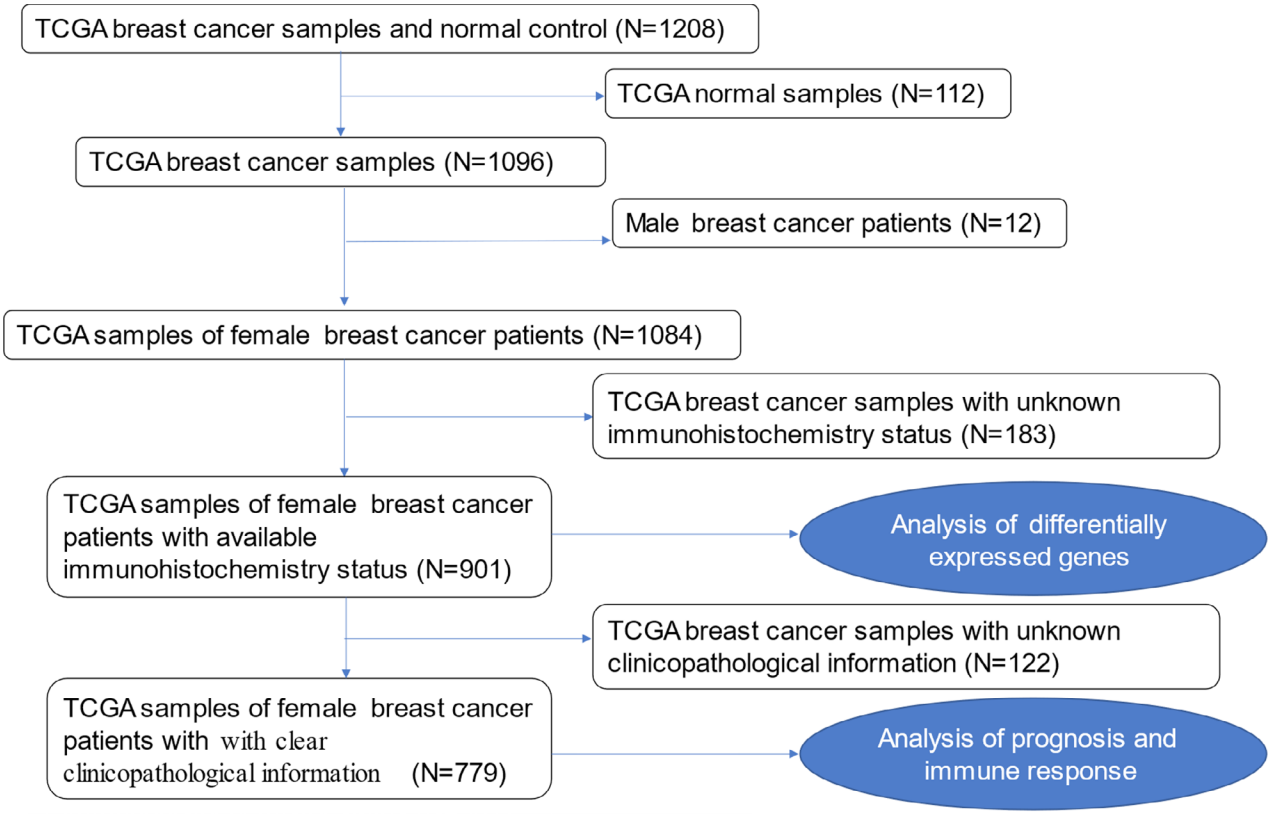

Supplementary Figure 1. Flow diagram of included TCGA female breast cancer samples with available immunohistochemistry status and clear clinicopathological information for further analysis.

TCGA, The Cancer Genome Atlas

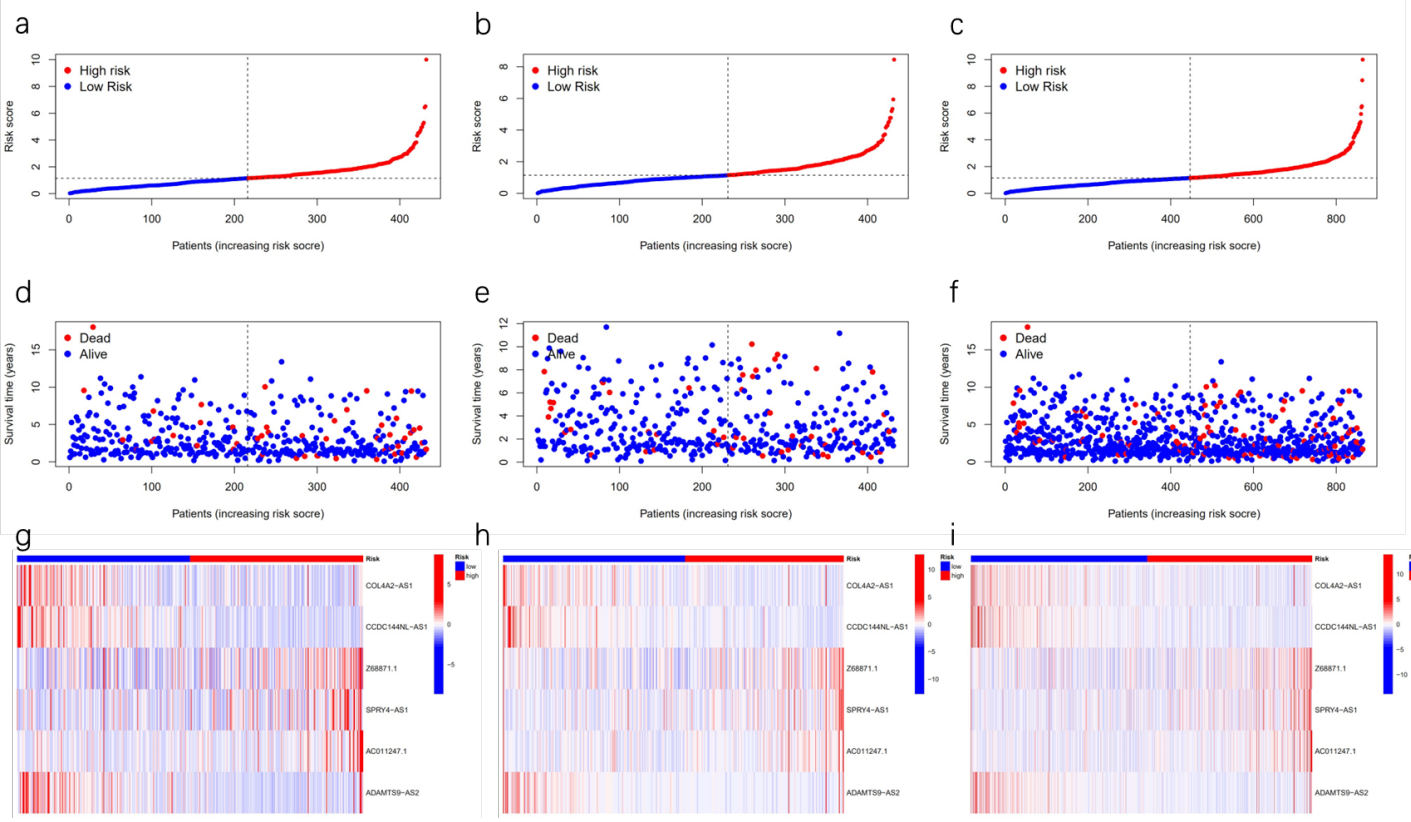

Supplementary Figure 2. Basic characteristics, survival analysis, and prognostic lncRNA of risk model. (a-c) Distribution of risk score in training (a), testing (b), and entire sample set (c); (d-f) Illustration of survival time and end-point vital status of patients in training (d), testing (e), and entire sample set (f); (g-i) heatmap of expression of six prognostic lncRNAs in high-risk and low-risk group from training (g), testing (h), and entire sample set (i).